

# Spectrum Shaping Methods for Predictive Control Approaches Applied to a Grid-Connected Power Electronics Converter

Benjamin Stickan, Per Rutquist, Tobias Geyer and Moritz Diehl

**Abstract**— This work proposes methods to incorporate penalties on specific frequency components of the output signal into a Model Predictive Control (MPC) problem formulation. This is relevant for many control applications, in which the control objectives are specified in the time domain (e.g. tracking), as well as in the frequency domain to shape the output spectrum of the system. Focusing on a grid-connected converter system, the objective function of Finite Control Set MPC is augmented by spectral penalties to shape the harmonic spectrum of the converter current.

## I. INTRODUCTION

When evaluating the quality of a feedback system, one often analyses the frequency spectra of its outputs. This can be achieved by sampling the output signals at a certain frequency, store the values for an adequate amount of time and perform a Discrete Fourier Transform (DFT) [1] on the data set. This transforms the signal from the time domain into the frequency domain. If the system has “desired” spectral components, but is prone to “undesired” components, the control engineer’s task is to remove these unwanted parts. It thus seems natural to integrate the DFT into the control objective to suppress undesired behavior in the first place.

### A. Model Predictive Control

One way of designing a feedback controller is Model Predictive Control (MPC) [2]. The basic idea is to use a scalar objective or “cost” function, which is a function of current and future system states and control inputs over a finite time horizon, and minimize it. For linear discrete-time systems it is common to use a quadratic cost function and to state the problem as a Quadratic Programming (QP) problem formulation. The solution to the problem is a control trajectory which can be applied to the system. To turn this into a feedback control law, a new QP can be set up and solved every time new system feedback (e.g. measurements) is available.

### B. Motivation

The application that motivates the presented work are power electronics converters that are connected to the public electricity network, from here on called *grid*. In most cases it

is desired that the converter injects only sinusoidal-shaped currents at the fundamental frequency (e.g. 50 Hz or 60 Hz) into the grid. All other frequencies are unwanted and thus there exist limits which the converter must meet. One challenge when controlling power electronics systems is that it is only possible to manipulate the states of the switches (e.g. IGBTs, MOSFETs, ...), which means the open-loop system input  $u$  can only attain values from a discrete set  $\mathbb{U}$ , resulting in a combinatorial optimization problem. Since this type is difficult to solve, it is common practice to solve the relaxed (averaged) problem [3], i.e. to solve for  $u \in \mathbb{R}^{n_u}$ , to add a modulation scheme, e.g. Pulse Width Modulation (PWM) or Space Vector Modulation (SVM) [4], and to apply the modulated signal to the system. A different approach is to directly control the switch positions. This is achieved by setting the controller sampling time much shorter than for the modulation-based approaches, and to define the switch positions to be constant throughout the sampling intervals. The optimal solution is then a future set of discrete switching states. In the context of MPC for power electronics, this is referred to as Finite Control Set Model Predictive Control (FCS-MPC) [5] [6]. In general, this approach leads to a high control dynamic, but also to a broad and uncontrolled output spectrum which often does not meet the strict grid requirements. Therefore, the main focus of this work is the efficient integration of a DFT into the QP problem.

### C. Spectral control

In [7], it was shown how spectral weights for distinct frequencies can be incorporated in a QP on the example of perception-based clipping of audio signals. In cases where only a small subset of the spectrum is to be manipulated, the concept of *Sliding DFT* [8] (SDFT) can be exploited. This is particularly efficient when the DFT window is much longer than the prediction horizon used for controlling the plant. In [9], the SDFT approach was implemented in a straight-forward enumeration scheme to control multilevel converters with a 1-step prediction horizon. As the SDFT can be regarded as a discrete-time filter, it is also possible to use any other discrete filter for the aforementioned approach. This is explained in [10] for a 3-level 3-phase converter. Related, yet more sophisticated approaches are described in [11], [12] and [13], where spectral weights as well as hard constraints are added to an MPC method. The DFT can be viewed as a filter that acts on the output of the system. In case of hard constraints on spectral components, recursive feasibility [14] has to be taken into account. In [15], the concept of *Dynamic Phasors* is utilized to

This work was supported by the German BMWi (0324166)  
Benjamin Stickan is with the Institute for Solar Energy Systems Freiburg, Germany [benjamin.stickan@ise.fraunhofer.de](mailto:benjamin.stickan@ise.fraunhofer.de)  
Per Rutquist is with the chair of Systems Control and Optimization, Department for Microsystems Engineering, University of Freiburg, Germany and Tomlab Software AB  
Moritz Diehl is with the chair of Systems Control and Optimization, Department for Microsystems Engineering, University of Freiburg, Germany  
Tobias Geyer is with ABB Corporate Research, 5405 Baden-Dättwil, Switzerland

more accurately model PWM based systems and therefore improve the control performance. The idea is to overcome the drawback of simple state-space averaged models, that cannot capture system dynamics in between to controller sampling instances, by generalizing them such that they also account for higher order harmonics. This in turn leads to a nonlinear relation between the input signals and the phasors.

#### D. Contribution

The work presented in the following will only address direct weighting of certain frequency components in the objective function of an MPC regulation problem, even though the concepts can be adopted for the spectral constraint case in a straight forward way. The novelty in comparison to existing work is the direct incorporation of a DFT, whereas previous work by [11], [12] and [13] generally describes how to utilize recursive filters for spectrum control in an MPC setting. The emphasis lies on efficient real-time capable algorithms for formulating dense unconstrained QPs, which can be used to implement fast linear feedback control laws. We propose three methods that result in the exact same closed-loop behavior but with possibly large differences in the computational complexity. It will be shown that for special cases, e.g. when the DFT window is much larger than the prediction horizon to capture very low frequencies or when only a few distinct frequencies are of interest, the computational effort can be significantly reduced by choosing the appropriate method. Therefore, detailed computation effort estimates are given and compared. Finally, the effectiveness of the proposed methods will be demonstrated for an FCS-MPC controlled converter.

## II. SPECTRUM PENALTIES IN THE OBJECTIVE FUNCTION

The Discrete Fourier Transform (DFT) matrix is given by

$$W = \frac{1}{\sqrt{L}} \begin{bmatrix} 1 & 1 & 1 & \dots & 1 \\ 1 & \omega & \omega^2 & \dots & \omega^{L-1} \\ 1 & \omega^2 & \omega^4 & \dots & \omega^{2(L-1)} \\ \vdots & \vdots & \vdots & \ddots & \vdots \\ 1 & \omega^{L-1} & \omega^{2(L-1)} & \dots & \omega^{(L-1)(L-1)} \end{bmatrix} \quad (1)$$

with  $\omega = e^{-\frac{2\pi j}{L}}$  ( $j$  being the imaginary unit) and  $L$  denoting the length of the signal. The scaling factor  $\frac{1}{\sqrt{L}}$  makes matrix  $W \in \mathbb{R}^{L \times L}$  unitary.

The DFT of a signal vector  $\bar{z} \in \mathbb{R}^L$  is then

$$W\bar{z} = p, \quad (2)$$

with  $p \in \mathbb{C}^L$ . In spectral shaping, it is desired to increase or decrease the magnitude of certain frequency components of  $p$ . The squared magnitude  $|p_h|^2$  for the  $h$ -th component of  $p$  allows us to define the objective-function term<sup>1</sup>

$$\mathcal{J} = \frac{1}{2} \sum_{h=0}^{L-1} q_h \cdot |p_h|^2 = \frac{1}{2} \bar{z}^H \underbrace{W^H Q_w W}_{:=Q} \bar{z}, \quad (3)$$

<sup>1</sup> $W^H$  denotes the Hermitian transpose of  $W$

with

$$Q_w = \begin{bmatrix} q_0 & 0 & \dots & 0 \\ 0 & q_1 & \dots & 0 \\ \vdots & \vdots & \ddots & \vdots \\ 0 & 0 & \dots & q_{L-1} \end{bmatrix} \quad (4)$$

and  $q_h \in \mathbb{R}^+$ . We also impose the following symmetry on all weights except for the DC component  $q_0$ :

$$q_h = q_{L-h}, \quad h = 1, \dots, \lceil L/2 \rceil - 1. \quad (5)$$

The reason is the following: for real-valued signals, the magnitudes of the positive and negative frequency components are the same. Therefore also the weights  $q_h$  may be symmetric. In a convex optimization problem setting, it is important to note that  $Q := W^H Q_w W$  is real, symmetric, circulant and positive definite. The proof can be found in [7].

## III. FULL SPECTRUM CONTROL

Within this section, we develop two dense problem formulations that both integrate a full spectrum DFT into an MPC regulation problem. Therefore, it is referred to as *Full Spectrum Control*.

We consider a linear discrete-time system of the form

$$x_{k+1} = Ax_k + Bu_k \quad (6)$$

$$z_k = Cx_k \quad (7)$$

with system states  $x_k \in \mathbb{R}^{n_x}$  and system inputs  $u_k \in \mathbb{R}^{n_u}$ . The system is also assumed to be stabilizable. To simplify the setting, the output  $z_k \in \mathbb{R}$  whose spectrum we aim to influence is assumed to be scalar. The MPC regulation problem, to which we want to add spectral penalties, is stated as the following discrete-time optimal control problem (OCP):

$$\begin{aligned} \min_{x_0, \dots, x_N, u_0, \dots, u_{N-1}} & \frac{1}{2} \sum_{k=0}^{N-1} (x_k^T Q x_k + u_k^T R u_k) + \frac{1}{2} x_N^T Q_N x_N \\ \text{s.t.} & \quad x_0 = \hat{x}_0, \\ & \quad x_{k+1} = Ax_k + Bu_k, \quad k = 0, \dots, N-1, \\ & \quad z_k = Cx_k, \quad k = 1, \dots, N, \end{aligned} \quad (8)$$

where  $Q, R, Q_N \succeq 0$ .

#### A. Problem formulation for $L = N$

In case the prediction horizon  $N$  equals the DFT filter length  $L$ , we can directly add the weighted objective function term  $\mathcal{J}$  to our existing problem (8). For convenience, we will join all states, inputs and outputs into respective vectors, in the following referred to as “stacking”, and use a matrix formulation to state the optimization problem (see e.g. [16]):

$$\begin{aligned} \min_{\bar{x}, \bar{u}, \bar{z}} & \frac{1}{2} (\bar{x}^T \bar{Q} \bar{x} + \bar{u}^T \bar{R} \bar{u} + \bar{z}^T \bar{Q} \bar{z}) \\ \text{s.t.} & \quad \bar{A} \bar{x} = \bar{B} \bar{u} + \bar{b}, \\ & \quad \bar{z} = \bar{C} \bar{x}, \end{aligned} \quad (9)$$

where

$$\bar{x} = [x_0^\top \ x_1^\top \ \cdots \ x_N^\top]^\top, \quad (10)$$

$$\bar{z} = [z_1^\top \ z_2^\top \ \cdots \ z_N^\top]^\top, \quad (11)$$

$$\bar{u} = [u_0^\top \ u_1^\top \ \cdots \ u_{N-1}^\top]^\top. \quad (12)$$

The equivalent problem after condensing, i.e. eliminating  $\bar{x}$  and  $\bar{z}$  using all equality constraints, is of the general form

$$\min_{\bar{u}} \frac{1}{2} \bar{u}^\top \mathbf{H} \bar{u} + \mathbf{g}^\top \bar{u} + \rho, \quad (13)$$

with  $\mathbf{H} \in \mathbb{R}^{n_u \times n_u}$  being the Hessian and  $\mathbf{g} \in \mathbb{R}^{n_u \times n_x N}$ . In this case, it can be written as

$$\min_{\bar{u}} \frac{1}{2} \bar{u}^\top (\bar{H} + D) \bar{u} + ((\bar{g}_b + d_b) \bar{b})^\top \bar{u} + \rho, \quad (14)$$

where

$$\bar{H} = (\bar{A}^{-1} \bar{B})^\top \bar{Q} \bar{A}^{-1} \bar{B} + \bar{R}, \quad (15)$$

$$D = (\bar{C} \bar{A}^{-1} \bar{B})^\top \bar{Q} \bar{C} \bar{A}^{-1} \bar{B}, \quad (16)$$

$$d_b = (\bar{C} \bar{A}^{-1} \bar{B})^\top \bar{Q} \bar{C} \bar{A}^{-1}, \quad (17)$$

$$\bar{g}_b = (\bar{A}^{-1} \bar{B})^\top \bar{Q} \bar{A}^{-1}. \quad (18)$$

Here,  $\bar{H} \in \mathbb{R}^{n_u \times n_u}$  denotes the Hessian of the original OCP to which we add the spectral weighting Hessian  $D \in \mathbb{R}^{n_u \times n_u}$ . Matrices  $\bar{g}_b \in \mathbb{R}^{n_u \times n_x N}$  and  $d_b \in \mathbb{R}^{n_u \times n_x N}$  are multiplied by the parameter vector  $\bar{b}$  to obtain  $\mathbf{g}$ . The remaining constant factor  $\rho$  will not change the solution of (14) and can thus be neglected, which is why we do not elaborate on it here.

From the above formula it can be seen that including spectral weights does not alter the complexity of solving an unconstrained (dense) quadratic MPC regulation problem in the case of  $L = N$ . Note, however, that the unconstrained problem (9) loses most of its sparse structure due to  $\bar{Q}$ , such that block sparse QP solvers such as FORCES [17] or qpDUNES [18] cannot be used.

### B. Problem formulation for $L > N$

In most control applications, it might be desirable to use filter lengths longer than the prediction horizon ( $L > N$ ). E.g. when the (controlled) output shows low frequency oscillations that cannot be captured by a DFT over the prediction horizon  $N$ . In this case,  $L$  can be expanded into the past such that

$$\bar{z} = \underbrace{[z_{N-L+1} \ \cdots \ z_0]}_{:= \bar{z}_p \text{ (past)}} \underbrace{[z_1 \ \cdots \ z_N]}_{:= \bar{z}_f \text{ (future)}}^\top, \quad (19)$$

where  $\bar{z}_p$  and  $\bar{z}_f$  are the past and future outputs of the system. In the context of a receding horizon control policy, we assume that we have access to the past outputs. E.g. they are stored in memory during the past control steps. We can

then rewrite (3) as

$$\begin{aligned} \mathcal{J} &= \frac{1}{2} \bar{z}^\top \bar{Q} \bar{z}, = \frac{1}{2} \begin{bmatrix} \bar{z}_p \\ \bar{z}_f \end{bmatrix}^\top \begin{bmatrix} \bar{Q}_p & \bar{Q}_{pf} \\ \bar{Q}_{pf}^\top & \bar{Q}_f \end{bmatrix} \begin{bmatrix} \bar{z}_p \\ \bar{z}_f \end{bmatrix} \\ &= \frac{1}{2} \bar{z}_f^\top \bar{Q}_f \bar{z}_f + \bar{z}_p^\top \bar{Q}_{pf} \bar{z}_f + \frac{1}{2} \bar{z}_p^\top \bar{Q}_p \bar{z}_p. \end{aligned} \quad (20)$$

Substituting this in (9) leads to the optimization problem

$$\begin{aligned} \min_{\bar{x}, \bar{u}, \bar{z}_f} \quad & \frac{1}{2} (\bar{x}^\top \bar{Q} \bar{x} + \bar{u}^\top \bar{R} \bar{u} + \bar{z}_f^\top \bar{Q}_f \bar{z}_f) + \bar{z}_p^\top \bar{Q}_{pf} \bar{z}_f \\ \text{s.t.} \quad & \bar{A} \bar{x} = \bar{B} \bar{u} + \bar{b}, \\ & \bar{z}_f = \bar{C} \bar{x}, \\ & \bar{z}_p = \hat{\bar{z}}_p \end{aligned} \quad (21)$$

with  $\hat{\bar{z}}_p \in \mathbb{R}^{L-N}$  being the vector of past outputs. The equivalent dense problem then reads as

$$\min_{\bar{u}} \frac{1}{2} \bar{u}^\top (\bar{H} + D) \bar{u} + ((\bar{g}_b + d_b) \bar{b} + d_{z_p} \hat{\bar{z}}_p)^\top \bar{u}, \quad (22)$$

with

$$d_{z_p} = (\bar{Q}_{pf} \bar{C} \bar{A}^{-1} \bar{B})^\top. \quad (23)$$

From (22) it can be seen that enlarging the filter length into the past requires the additional multiplication of  $d_{z_p} \in \mathbb{R}^{n_u \times (L-N)}$  with  $\hat{\bar{z}}_p \in \mathbb{R}^{L-N}$  to obtain  $\mathbf{g}$ .

## IV. PARTIAL SPECTRUM CONTROL

In some applications it is desired to have a huge filter size but short prediction horizon, where only a small range of the spectrum or even only one component is of interest. This can be exploited to reduce the computational effort of the overall control algorithm. Instead of setting  $q_h = 0$  for all disregarded frequencies in the *Full Spectrum Control* method, we aim at algorithms which require less computational effort and deliver the same solution. In this section, we will derive dynamic system interpretations of such a partial DFT and develop two methods how to incorporate them into the unconstrained problem formulation. Because only a subset of the full spectrum is of interest here, we refer to these methods as *Partial Spectrum Control* methods.

A well known method for calculating single frequency components at only a fraction of the computational cost of a full DFT is the Sliding DFT [8] algorithm, which we use to start our derivation. The  $h$ -th spectral component  $p_h$  from (2) at time step  $k$  over the past  $L$  signal samples is calculated by

$$\begin{aligned} p_{h,k} &= \frac{1}{\sqrt{L}} \sum_{n=1-L}^0 z_{k+n} \omega^{(n-1)h} \\ &= \frac{1}{\sqrt{L}} \left( z_{k+1-L} + \sum_{n=2-L}^0 z_{k+n} \omega^{(n-1)h} \right), \end{aligned} \quad (24)$$

with  $h = 0, \dots, L - 1$ .

At time step  $k + 1$  we obtain

$$\begin{aligned}
p_{h,k+1} &= \frac{1}{\sqrt{L}} \sum_{n=1-L}^0 z_{k+1+n} \omega^{(n-1)h} \\
&= \frac{1}{\sqrt{L}} \sum_{n=2-L}^1 z_{k+n} \omega^{(n-2)h} \\
&= \frac{\omega^{-h}}{\sqrt{L}} \left( \sum_{n=2-L}^0 z_{k+n} \omega^{(n-1)h} + z_{k+1} \underbrace{\omega^{Lh}}_{=1} \right) \\
&= \omega^{-h} \left( p_{h,k} + \frac{z_{k+1}}{\sqrt{L}} - \frac{z_{k+1-L}}{\sqrt{L}} \right), \quad (25)
\end{aligned}$$

which shows that the spectral component of the next time step can be recursively calculated from the previous one. It can be interpreted as adding the new value  $z_{k+1}$  to the DFT window and removing the last value  $z_{k+1-L}$ . To avoid the necessity for complex calculations, we propose to use a vector representation of complex numbers. We define the function

$$\gamma : \mathbb{C} \rightarrow \mathbb{R}^2, x \mapsto \begin{bmatrix} \operatorname{Re}(x) \\ \operatorname{Im}(x) \end{bmatrix}, \quad (26)$$

the filter-state

$$s_{h,k} := \gamma(p_{h,k}) \quad (27)$$

and matrices

$$\begin{aligned}
A_{s,h} &= \begin{bmatrix} \operatorname{Re}(\omega^{-h}) & -\operatorname{Im}(\omega^{-h}) \\ \operatorname{Im}(\omega^{-h}) & \operatorname{Re}(\omega^{-h}) \end{bmatrix} \\
&= \begin{bmatrix} \cos(2\pi h/L) & -\sin(2\pi h/L) \\ \sin(2\pi h/L) & \cos(2\pi h/L) \end{bmatrix}, \quad (28)
\end{aligned}$$

$$B_{s,h} = \frac{1}{\sqrt{L}} \begin{bmatrix} \operatorname{Re}(\omega^{-h}) \\ \operatorname{Im}(\omega^{-h}) \end{bmatrix} = \frac{1}{\sqrt{L}} \begin{bmatrix} \cos(2\pi h/L) \\ \sin(2\pi h/L) \end{bmatrix}, \quad (29)$$

such that

$$s_{h,k+1} = A_{s,h} s_{h,k} + B_{s,h} (z_{k+1} - z_{k+1-L}). \quad (30)$$

We now have defined a recursive DFT formula that can be viewed as a dynamic system equation. It is easy to see that  $A_{s,h}$ , which we identify as the system matrix, is a rotational matrix, and the elements of  $B_{s,h}$  are exactly the same as in the first column of  $A_{s,h}$  multiplied by a constant. From a computational complexity point of view this is not the preferred form, but it simplifies the integration into the MPC problem formulation.

Equation (30) now serves a dual purpose:

- 1) It can be used as a filter-like structure to recursively calculate the current value of any single spectral component at each time step.
- 2) State  $s_h$  can be incorporated into the MPC formulation to control the spectral behavior.

#### A. Recursive partial DFT

As in the previous sections, we aim to derive a quadratic objective function term to weight the absolute value of the spectral components with a real-valued factor.

*Lemma 1:* We can express the weighted squared magnitude of the  $h$ -th spectral component at time step  $k$  by the DFT filter state as follows:

$$q_h |p_{h,k}|^2 = s_{h,k}^\top Q_{s,h} s_{h,k} \quad (31)$$

$$\text{with } Q_{s,h} = \begin{bmatrix} q_h & 0 \\ 0 & q_h \end{bmatrix}. \quad (32)$$

*Proof:* We can write  $p_{h,k}$  as

$$\begin{aligned}
p_{h,k} &= \operatorname{Re}(p_{h,k}) + j \operatorname{Im}(p_{h,k}) \\
&= s_{h,k,1} + j s_{h,k,2} \quad (33)
\end{aligned}$$

with  $j$  being the imaginary unit and thus have

$$q_h |p_{h,k}|^2 = s_{h,k}^\top Q_{s,h} s_{h,k} \quad (34)$$

To ensure the same solution for the *Full* as well as for the *Partial Spectrum Control* methods, we suppose that at current time step  $k$  we want to optimize over  $N$  future system outputs  $(z_{k+1}, \dots, z_{k+N})$ , such that the objective function does not contain intermediate states  $(s_{k+1}, \dots, s_{k+N-1})$  but only the final state  $s_{k+N}$ . Assuming that we want to add weights on multiple frequency components  $h \in S \subseteq \{0, \dots, L - 1\}$  to (8) by utilizing the recursive DFT formulation (30), we can state our problem as

$$\begin{aligned}
\min_{\substack{x_0, \dots, x_N \\ u_0, \dots, u_{N-1} \\ s_{h,N}, h \in S}} & \frac{1}{2} \sum_{k=0}^{N-1} (x_k^\top Q x_k + u_k^\top R u_k) \\
& + \frac{1}{2} x_N^\top Q_N x_N + \sum_{h \in S} s_{h,N}^\top Q_{s,h} s_{h,N} \\
\text{s.t.} & \quad x_0 = \hat{x}_0, \\
& \quad x_{k+1} = A x_k + B u_k, \quad k = 0, \dots, N - 1, \\
& \quad z_k = C x_k, \quad k = 1, \dots, N, \\
& \quad s_{h,0} = \hat{s}_{h,0}, \quad h \in S, \\
& \quad s_{h,k+1} = A_{s,h} s_{h,k} \quad k = 0, \dots, N - 1, \\
& \quad + B_{s,h} (z_{k+1} - z_{k+1-L}), \quad h \in S, \quad (35)
\end{aligned}$$

where the initial filter state  $\hat{s}_0$  is calculated recursively with (30) at each time step. The dense problem then becomes

$$\begin{aligned}
\min_{\bar{u}} & \frac{1}{2} \bar{u}^\top (\bar{H} + D) \bar{u} \\
& + ((\bar{g}_b + d_b) \bar{b} + d_{z_{pN}} \bar{z}_{pN} + d_{s_0} \bar{s}_0)^\top \bar{u}, \quad (36)
\end{aligned}$$

where

$$d_{z_{pN}} = (\bar{C} \bar{A}^{-1} \bar{B})^\top (\bar{A}_s^{-1} \bar{B}_s)^\top Q \bar{A}_s^{-1} \bar{B}_s, \quad (37)$$

$$d_{s_0} = (\bar{C} \bar{A}^{-1} \bar{B})^\top (\bar{A}_s^{-1} \bar{B}_s)^\top Q \bar{A}_s^{-1}, \quad (38)$$

Here,  $\bar{z}_{pN} = [z_{-L+1} \ \dots \ z_{-L+N}]^\top$  for  $L > N$  denotes a set of  $N$  past output values and  $\bar{s}_0 \in \mathbb{R}^{2n_h}$  with  $n_h = |S|$  is the vector of all stacked initial filter states  $\hat{s}_{h,0}$ . Matrices  $\bar{A}_s \in \mathbb{R}^{2n_h \times 2n_h}$  and  $\bar{B}_s \in \mathbb{R}^{2n_h}$  contain all  $A_{s,h}$  and  $B_{s,h}$ . Note that, independent of  $N$ , this method always requires to store the past  $L$  system outputs.

### B. Improved recursive partial DFT

To further reduce the computation time (in most cases), a combination of two different recursive formulas, one for the filter and another one for the optimization problem formulation, can be utilized. The purpose of the following is to eliminate the  $d_{zpN} \bar{z}_{pN}$  term in (36), such that the dense optimization problem becomes easier to formulate.

*Lemma 2:* Inside the OCP formulation the simplified recursion

$$\tilde{s}_{h,k+1} = A_{s,h} \tilde{s}_{h,k} + B_{s,h} z_{k+1}, \quad k = 0, \dots, N-1 \quad (39)$$

can be used, if the modified recursive filter rule

$$v_{h,k+1} = A_{s,h} v_{h,k} + B_{s,h} z_{k+1} - \tilde{B}_{s,h} z_{k+1-L+N}, \quad k = -\infty, \dots, 0 \quad (40)$$

$$\text{with } \tilde{B}_{s,h} = A_{s,h}^{-N} B_{s,h} \quad (41)$$

is applied. When we set the initial filter of the OCP to  $\tilde{s}_{h,0} = v_{h,0}$ , then

$$s_{h,N} = \tilde{s}_{h,N} \quad (42)$$

still holds at the end of the prediction horizon.

*Proof:* First, we write the original recursion as the sum (see (24)-(30) and note that we changed the index to simplify notation):

$$\begin{aligned} s_{h,k} &= A_{s,h} s_{h,k-1} + B_{s,h} (z_k - z_{k-L}) \\ &= \sum_{n=k+1-L}^k A_{s,h}^{k-n} B_{s,h} z_n. \end{aligned} \quad (43)$$

We do the same for the modified filter:

$$\begin{aligned} v_{h,k} &= A_{s,h} v_{h,k-1} + B_{s,h} z_{s,k} - \tilde{B}_{s,h} z_{k-L+N} \\ &= \sum_{n=k+N+1-L}^k A_{s,h}^{k-n} B_{s,h} z_n. \end{aligned} \quad (44)$$

Starting at  $\tilde{s}_{h,0} = v_{h,0}$ , the final filter state within the prediction horizon can be calculated as

$$\begin{aligned} \tilde{s}_{h,N} &= \sum_{n=1}^N A_{s,h}^{N-n} B_{s,h} z_n + A_{s,h}^N v_{h,0} \\ \tilde{s}_{h,N} &= \sum_{n=1}^N A_{s,h}^{N-n} B_{s,h} z_n + A_{s,h}^N \sum_{n=N+1-L}^0 A_{s,h}^{-n} B_{s,h} z_n \\ &= \sum_{n=N+1-L}^N A_{s,h}^{N-n} B_{s,h} z_n = s_{h,N}. \end{aligned} \quad (45)$$

Analogously to (35) and (36) we write the problem as:

$$\begin{aligned} \min_{\substack{x_0, \dots, x_N \\ u_0, \dots, u_{N-1} \\ \tilde{s}_{h,N}, h \in S}} & \frac{1}{2} \sum_{k=0}^{N-1} (x_k^T Q x_k + u_k^T R u_k) \\ & + \frac{1}{2} x_N^T Q_N x_N + \sum_{h \in S} \tilde{s}_{h,N}^T Q_{s,h} \tilde{s}_{h,N} \\ \text{s.t.} & \quad x_0 = \hat{x}_0, \\ & \quad x_{k+1} = A x_k + B u_k, \quad k = 0, \dots, N-1, \\ & \quad z_k = C x_k, \quad k = 1, \dots, N, \\ & \quad \tilde{s}_{h,0} = v_{h,0} \quad h \in S, \\ & \quad \tilde{s}_{h,k+1} = A_{s,h} \tilde{s}_{h,k} \quad k = 0, \dots, N-1, \\ & \quad \quad \quad + B_{s,h} z_{k+1}, \quad h \in S \end{aligned} \quad (46)$$

and obtain the dense problem

$$\min_{\bar{u}} \frac{1}{2} \bar{u}^T (\bar{H} + D) \bar{u} + ((\bar{g}_b + d_b) \bar{b} + d_{s_0} \bar{s}_0)^T \bar{u}. \quad (47)$$

This results in a cheaper dense formulation algorithm for the optimization problem with the side effect of having a slightly more expensive recursive filter rule (30) compared to original filter equation (40).

### V. COMPUTATIONAL BURDEN

In this section, we will compare the ‘‘full spectrum’’, ‘‘partial’’ and ‘‘improved partial’’ methods regarding the computational efficiency over the following parameters:

- $N$ : Horizon length
- $L$ : Filter length
- $n_h$ : Number of frequency components

Incorporating spectral shaping penalties into the dense unconstrained MPC problem requires changing the Hessian as well as the vector  $\mathbf{g}$  of the problem. Since the problem considered here is linear, the Hessian remains constant in the dense problems (22), (36) and (47). In contrast to that,  $\mathbf{g}$  needs to be recalculated at each time step according to the initial states and parameters.

When we revise the dense problem (22), we see that adding  $D$  to  $\bar{H}$  and  $d_b$  to  $\bar{g}_b$  does not change the problem complexity. Only the multiplication of the additional parameter vector  $\bar{z}_p$  by  $d_{zp}$  increases the effort of calculating  $\mathbf{g}$ . Since the Hessian is not affected, we only elaborate on additional computations that are necessary for calculating  $\mathbf{g}$  and the DFT filter in the following.

Table I summarizes the necessary additional operations for each method while Table II gives the corresponding matrix dimensions. To get an estimate on the computational effort, we assume that a vector-vector multiplication of vectors of length  $m$  requires  $m$  multiplications and  $m-1$  additions, resulting in  $2m-1$  flops. A matrix-vector multiplication with an  $n \times m$  matrix leads to  $n(2m-1)$  flops accordingly. Adding two vectors of length  $m$  requires  $m$  additions.

- Fig. 1 compares the effort of all three methods (A: ‘‘full’’, B: ‘‘partial’’, C: ‘‘improved partial’’) depending on the

TABLE I

ADDITIONAL OPERATIONS REQUIRED AT EACH TIME STEP COMPARED TO THE MPC METHOD WITHOUT SPECTRUM CONTROL

Method		g	$h$ -th component DFT filter
A	Full spectrum control	$d_{zp} \bar{z}_p$	-
B	Partial spectrum control	$d_{s0} \bar{s}_0$ $+ d_{zpN} \bar{z}_{pN}$	$A_{s,h} s_{h,k}$ $+ B_{s,h} (z_{k+1} - z_{k+1-L})$
C	Improved partial spectrum control	$d_{s0} \bar{s}_0$	$A_{s,h} v_{h,k} + B_{s,h} z_{k+1}$ $- \tilde{B}_{s,h} z_{k+1-L+N}$

TABLE II  
MATRIX DIMENSIONS

Method A	$d_{zp} \in \mathbb{R}^{N \times (L-N)}$	
Method B	$d_{s0} \in \mathbb{R}^{N \times 2n_h}$ , $A_{s,h} \in \mathbb{R}^{2 \times 2}$	$d_{zpN} \in \mathbb{R}^{N \times N}$ , $B_{s,h} \in \mathbb{R}^{2 \times 1}$
Method C	$d_{s0} \in \mathbb{R}^{N \times 2n_h}$ , $B_{s,h} \in \mathbb{R}^{2 \times 1}$	$A_{s,h} \in \mathbb{R}^{2 \times 2}$ , $\tilde{B}_{s,h} \in \mathbb{R}^{2 \times 1}$

prediction horizon length  $N$ . It shows the relation between the number of future and past DFT window values for a fixed window size. Method (C) does only depend on  $N$  via  $d_{s0}$  and thus the effort grows linearly. Method (B) contains  $d_{zpN} \in \mathbb{R}^{N \times N}$  such that its flop count grows quadratically, whereas (A) is a negative quadratic function.

Fig. 2 compares the methods over the number of frequencies that are penalized. Method (A) has constant complexity over  $n_h$ , because it always penalizes all frequencies, just that the penalty for the non-regarded frequencies is set to zero. Methods (B) and (C) have a linear increase with different slopes, such that it depends on the  $N/L$  ratio if the complexity curves intersect. It thus depends on the specific problem parameters which method suits best.

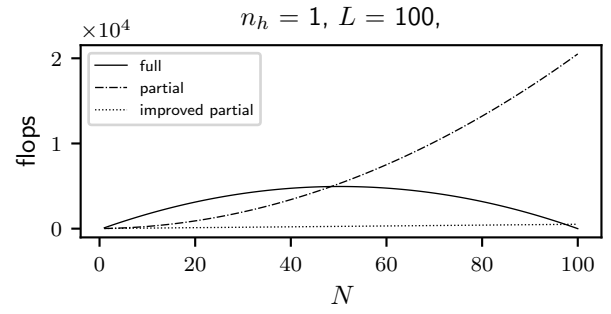
## VI. RESULTS

As mentioned in the beginning, the original target system, of which we aim to control the output spectrum, is a grid-connected FCS-MPC controlled 3-level Neutral Point Clamped (NPC) converter. The topology is shown in Fig. 3. The following continuous-time state-space model has been used for the simulations as well as for the controller design:

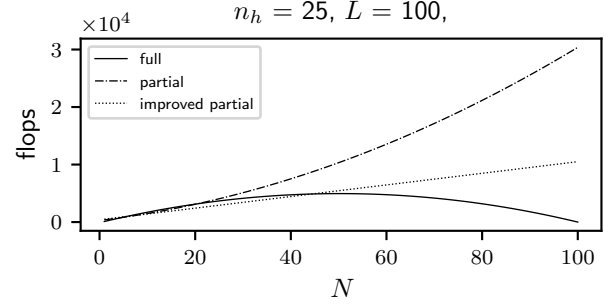
$$F = \begin{bmatrix} \frac{R}{X} & 0 & -\frac{1}{X} & 0 \\ 0 & \frac{R}{X} & 0 & -\frac{1}{X} \\ 0 & 0 & 0 & -\omega_g \\ 0 & 0 & \omega_g & 0 \end{bmatrix}, G = \begin{bmatrix} \frac{V_{DC}}{2X} & 0 \\ 0 & \frac{V_{DC}}{2X} \\ 0 & 0 \\ 0 & 0 \end{bmatrix} K, \quad (48)$$

$$\text{with } K = \frac{2}{3} \begin{bmatrix} 1 & -0.5 & -0.5 \\ 0 & \frac{\sqrt{3}}{2} & -\frac{\sqrt{3}}{2} \end{bmatrix}.$$

$F \in \mathbb{R}^{4 \times 4}$  denotes the system matrix,  $G \in \mathbb{R}^{4 \times 3}$  is the input matrix and  $K \in \mathbb{R}^{2 \times 3}$  is the Clarke transform matrix. The state vector  $x = [i_\alpha \ i_\beta \ v_{g,\alpha} \ v_{g,\beta}]^T$  contains converter-side currents and the grid voltages whereas the input vector  $u = [u_a \ u_b \ u_c]^T \in \{-1, 1\}^3$  relates to the switch posi-



(a) Single frequency penalization.



(b) Penalization of 25 distinct frequencies.

Fig. 1. Computational effort for all three methods over the prediction horizon  $N$  with the fixed DFT window length  $L = 100$ .

tions a 3-phase 3-level converter can generate. All quantities are given in the per unit (pu) system in Table III.

### A. FCS-MPC problem

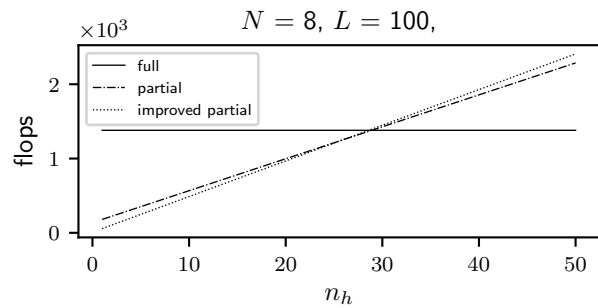
The MPC problem formulation is of combinatorial type, because the system inputs  $u$  are restricted to a discrete set. The control approach used in this work first solves the relaxed (unconstrained) problem. Afterwards, a sphere decoding algorithm is used to determine the optimal discrete inputs to the system. We incorporated the spectrum shaping penalties with the “improved partial control” method into the relaxed problem formulation. For a more detailed description of the FCS-MPC method and sphere decoding, see e.g. [19].

### B. Simulation settings

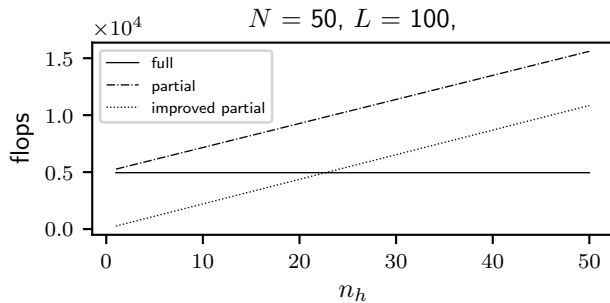
To evaluate the effectiveness of the spectrum shaping algorithms, two scenarios were simulated; one without and another one with spectrum control on both the converter currents  $i_\alpha$  and  $i_\beta$ . The average switching frequency was manually tuned, in both cases, to approximately 500 Hz by a delta penalty on the switching actions. Parameters of the simulation can be found in Table III. The system has been simulated for 1 s using MATLAB Simulink. The output current  $i_\alpha$  was recorded at 40 kHz and afterwards transformed to the frequency domain. Blanking times that prevent shoot-through of the switches were not considered.

### C. Discussion

All presented spectrum control methods deliver the same results and only differ in their computational complexity.



(a) Short horizon with  $N = 8$ .



(b) Long horizon with  $N = 50$ .

Fig. 2. Computational effort for all three methods over the number of frequencies to be penalized with fixed DFT window length  $L = 100$ .

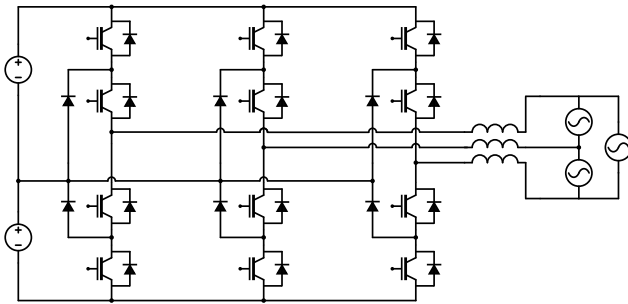


Fig. 3. Circuit diagram of the investigated 3-level NPC converter topology.

Fig. 4 shows the critical part of the spectrum of  $i_\alpha$  for both scenarios as well as the harmonic limits given in the IEEE 519 guideline. Fig. 4a shows many violations on the harmonic distortion limits especially for even harmonics, which are only allowed to be  $1/4$  of the odd ones. For the spectrum shown in Fig. 4b, we implemented penalties on harmonics of the order  $h = 20 \dots 60$  and penalized the even ones 2.5 times more than the odd ones. It can be seen that there are significantly fewer violations and that even-order harmonic components are reduced to a minimum. As a result, the grid code limits are mostly met. This widens the application range for model predictive controllers not only to grid-connected converters, but also to many other systems that need to meet criteria in the frequency domain.

## VII. CONCLUSION

It has been shown how penalties on certain components in the frequency domain can be incorporated into a quadratic

TABLE III  
SYSTEM PARAMETERS

$V_{ll,r}$	3300 V	rated line-to-line rms voltage
$S_r$	9 MVA	rated apparent power
$I_r$	$\frac{S_r}{\sqrt{3}V_{ll,r}}$	rated rms phase current
$f_{1,r}$	50 Hz	rated fundamental frequency
$\omega_b$	$2\pi f_{1,r}$	base angular frequency
$V_b$	$\sqrt{\frac{2}{3}}V_{ll,r}$	base voltage
$I_b$	$\sqrt{2}I_r$	base current
$\omega_g$	1	angular grid frequency [pu]
$X$	0.15	grid reactance [pu]
$R$	0.015	grid resistance [pu]
$V_{DC}$	$\frac{5200 \text{ V}}{V_b}$	DC-link voltage [pu]
$T_{s,r}$	25 $\mu\text{s}$	controller sampling interval [SI]
$T_s$	$\omega_b T_{s,r}$	controller sampling interval [pu]
$T_{sim}$	1 s	simulation time
$f_{dft}$	40 kHz	sampling frequency of DFT on system output
$L$	800	DFT window length inside controller
$N$	3	MPC prediction horizon

MPC problem formulation. Three different methods have been developed that all lead to the same system behavior, but with different execution costs. It thus depends on the problem structure which method suits best. Parameters to be considered are the number of harmonics  $n_h$  to be penalized, the MPC prediction horizon  $N$  and the filter length  $L$  which relates to the lowest harmonic. Practical limitations to be considered are the amount of past data that needs to be stored and numeric errors which might propagate and/or accumulate in the recursive filter based methods. The practical relevance of this method was demonstrated for an FCS-MPC controlled grid-connected converter. FCS-MPC achieves a superior dynamic performance but suffers from an output spectrum that is non-compliant with common grid regulations. After adding spectrum penalties, limits on harmonic current distortions are shown to be mostly met.

## REFERENCES

- [1] L. Homssi and A. Despujols. Fourier series expansion and DFT on a moving window. In *[Proceedings] IECON '90: 16th Annual Conference of IEEE Industrial Electronics Society*, pages 363–367 vol.1, Nov 1990.
- [2] J. Rawlings, D. Mayne, and M. Diehl. *Model predictive control : theory, computation, and design, 2nd Edition*. Nob Hill Publishing, Madison, Wisconsin, 2017.
- [3] R. D. Middlebrook and S. Cuk. A general unified approach to modelling switching-converter power stages. In *1976 IEEE Power Electronics Specialists Conference*, pages 18–34, June 1976.
- [4] K. Zhou and D. Wang. Relationship Between Space-Vector Modulation and Three-Phase Carrier-Based PWM: A Comprehensive Analysis. *IEEE Trans. Industrial Electronics*, 49:186–196, 2002.
- [5] T. Geyer and D. E. Quevedo. Multistep finite control set model predictive control for power electronics. *IEEE Transactions on Power Electronics*, 29(12):6836–6846, Dec 2014.
- [6] J. Rodriguez and P. Cortes. *Predictive control of power converters and electrical drives*. IEEE/Wiley, Chichester, West Sussex, UK Hoboken, N.J., 2012.
- [7] B. Defraene, T. van Waterschoot, H. J. Ferreau, M. Diehl, and M. Moonen. Real-time perception-based clipping of audio signals using convex optimization. *IEEE Transactions on Audio, Speech, and Language Processing*, 20(10):2657–2671, Dec 2012.

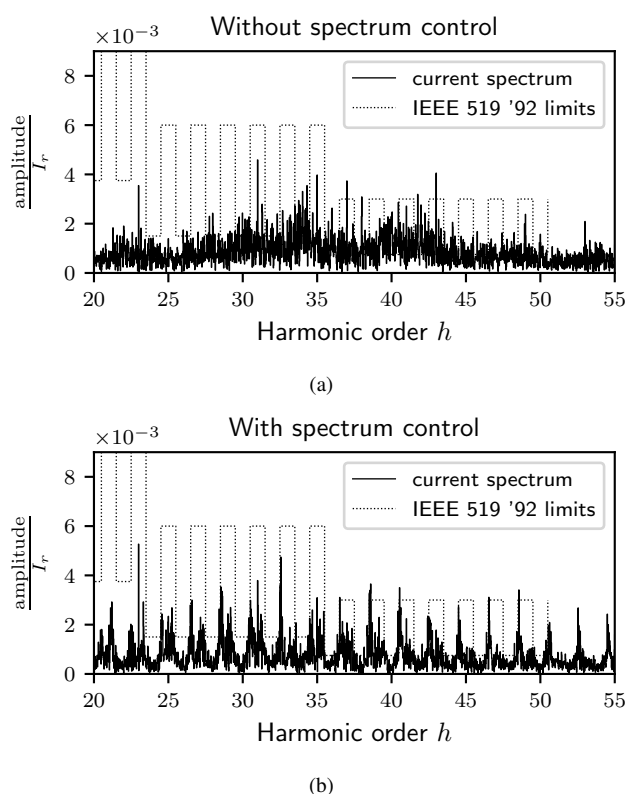


Fig. 4. Comparison of the spectrum of  $i_\alpha$  in per unit for an FCS-MPC controlled grid-connected converter without and with spectrum control.

- [8] E. Jacobsen and R. Lyons. The sliding DFT. *IEEE Signal Processing Magazine*, 20(2):74–80, March 2003.
- [9] S. Kouro, B. La Rocca, P. Cortes, S. Alepuz, B. Wu, and J. Rodriguez. Predictive control based selective harmonic elimination with low switching frequency for multilevel converters. In *2009 IEEE Energy Conversion Congress and Exposition*, pages 3130–3136, Sept 2009.
- [10] P. Cortes, J. Rodriguez, D. E. Quevedo, and C. Silva. Predictive current control strategy with imposed load current spectrum. *IEEE Transactions on Power Electronics*, 23(2):612–618, March 2008.
- [11] R. Gondhalekar, C. N. Jones, T. Besselmann, J. Hours, and M. Mercangöz. Constrained spectrum control using MPC. In *2011 50th IEEE Conference on Decision and Control and European Control Conference*, pages 1219–1226, Dec 2011.
- [12] J. Hours, M. N. Zeilinger, R. Gondhalekar, and C. N. Jones. Spectrogram-MPC: Enforcing hard constraints on systems' output spectra. In *2012 American Control Conference (ACC)*, pages 2010–2017, June 2012.
- [13] J. Hours, M. N. Zeilinger, R. Gondhalekar, and C. N. Jones. Constrained spectrum control. *IEEE Transactions on Automatic Control*, 60(7):1969–1974, July 2015.
- [14] J. Löfberg. Oops! I cannot do it again: Testing for recursive feasibility in MPC. *Automatica*, 48(3):550 – 555, 2012.
- [15] S. Almér, S. Mariéthoz, and M. Morari. Dynamic Phasor Model Predictive Control of Switched Mode Power Converters. *IEEE Transactions on Control Systems Technology*, 23(1):349–356, Jan 2015.
- [16] G. Frison. *Algorithms and Methods for Fast Model Predictive Control*. Dissertation, Technical University of Denmark, Department of Applied Mathematics and Computer Science, 2016.
- [17] A. Zanelli, A. Domahidi, J. Jerez, and M. Morari. Forces nlp: an efficient implementation of interior-point... methods for multistage nonlinear nonconvex programs. *International Journal of Control*, pages 1–17, 2017.
- [18] J. V. Frasch, S. Sager, and M. Diehl. A Parallel Quadratic Programming Method for Dynamic Optimization Problems. *Mathematical Programming Computation*, 2013. (submitted).
- [19] T. Geyer. *Model predictive control of high power converters and*